Self-Assembled Monolayers on Gold Nanoparticles**

Antonella Badia, Shanti Singh, Linette Demers, Louis Cuccia, G. Ronald Brown, and R. Bruce Lennox*

Abstract: Self-assembled monolayers (SAMs) of *n*-alkanethiolates on gold, silver, and copper have been intensively studied both as model organic surfaces and as modulators of metal surface properties. Sensitivity restrictions imposed by monolayer coverage and the low surface area of planar metal substrates, however, limit the characterization of these films in molecualar terms to surface enhancement techniques. As a result, key aspects such as film dynamics and alkyl chain ordering remain ill-defined. The characterization of the thermal behavior of SAMs is important not only for the design of stable, well-ordered organic superlattices, but also for the fundamental understanding of the factors that drive molecular interactions in two dimensions. Phase properties in SAMs have been addressed here through the synthesis of gold nanoparticles of 20–30 Å in diameter and fully covered with alkylthiol chains. These thiol-modified gold nanoparticles with large surface areas have enabled the monolayer film structure to be uniquely characterized by transmission FT-IR spectroscopy, NMR spectroscopy, and differential scanning calorimetry. Our studies reveal that for long-chain thiols ($\geq C_{16}$), the alkyl chains exist predominantly in an extended, all-*trans* ordered conformation at 25 °C. Furthermore, calorimetry, variable temperature transmission FT-IR spectroscopy, and solid-state ^{13}C NMR studies have established that a cooperative chain melting process occurs in these alkylated metal colloids. How this arises is not immediately evident, given the relation between the extended chain conformation and the geometry of the spherical nanoparticles. Transmission electron microscopy (TEM) reveals that adjacent gold particles are separated by approximately one chain length; this suggests that chain ordering arises from an interdigitation of chains on neighboring particles. The thermotropic behavior is sensitive to the alkyl chain length and chain packing density. The alkylated nanoparticles can thus serve as a highly dispersed analogue to the much-studied planar SAMs.

Keywords
alkylthiols · gold · nanoparticles · phase transitions · self-assembly

Introduction

The properties of organic molecules adsorbed on metal surfaces are of particular interest owing to the central role adsorbates play in catalysis, corrosion, and electrode processes. A number of studies, for example, have dealt with the structure and dynamics of monolayer (or sub-monolayer) coverage where the adsorbate is an aromatic heterocycle or *n*-alkylthiol.[1–3] To date, little is known about the organizational state of chains in self-assembled monolayers (SAMs) of the otherwise much-studied *n*-alkylthiols chemisorbed on gold (RS–Au). The conformational lability of alkyl chains introduces the possibility that order–disorder transitions analogous to the gel-to-liquid crystalline phase transitions observed in lipid assemblies may arise. A complex melting process which occurs within RS–Au SAMs has in fact been recently inferred by using both electrochemical and synchroton X-ray diffraction as reporting techniques.[4, 5] Of note in the former are the striking parallels between temperature-dependent ion fluxes in RS–Au SAMs and the phase-transition behavior of biomimetic lipid vesicles.[4]

In the following, we describe a characterization of the thermal properties of RSH-derivatized gold nanoparticles.[6] This system was chosen because of its obvious potential to serve as a high surface area analogue to SAMs formed on planar metal surfaces. Sensitivity restrictions imposed by monolayer coverage greatly hinder the application of techniques such as calorimetry and NMR to the study of planar SAMs. As a result, issues such as chain dynamics, adsorbate phase diagrams, and relaxation processes remain open and ill-defined at the present time. We are especially interested in chain ordering and disordering in monolayers, and how this interplay manifests itself as grain boundaries and defect sites. If SAMs are to be ultimately used in molecular electronic and optoelectronic devices, then their structural integrity must be thoroughly understood, in both kinetic and thermodynamic terms. To this end, we have characterized the thermal properties of RSH monolayer-coated gold nanoparticles in macroscopic (by calorimetry and transmission electron microscopy) and microscopic (by infrared and NMR spectroscopy) terms. We show that these SAMs show strong parallels to monolayers formed at planar surfaces, but also distinct differences become apparent due to the large radius of curvature of these spherical gold particles.

[*] Prof. R. B. Lennox, A. Badia, S. Singh, L. Demers, L. Cuccia, Prof. G. R. Brown
Department of Chemistry, McGill University
801 Sherbrooke Street West, Montreal, Quebec H3A 2K6 (Canada)
Fax: Int. code +(514)398-3797
e-mail: BruceLennox@maclan.mcgill.ca

[**] Presented in part at the 78th Canadian Society for Chemistry Conference and Exhibition, May 28–June 1, 1995, Guelph, Canada and at the 210th National Meeting of the American Chemical Society, Aug. 20–25, 1995, Chicago, Ill.

  0947-6539/96/0203-0359 $ 15.00+.25/0

Results and Discussion

Investigation of the phase properties of monolayer films requires particular precautions to ensure the purity of their preparation. After the initial synthesis, thin-layer chromatography (TLC) of the "recrystallized" colloidal particles shows the presence of free disulfide. Extensive washing with ethanol to remove unbound disulfide surfactant leads to a disulfide-free ^{1}H NMR spectrum of the RSH-derivatized gold, and TLC shows no trace of either labile thiol and/or disulfide. The ^{1}H and ^{13}C NMR resonances of the powders dispersed in solvent are considerably broadened for the RS–Au nanoparticles as compared to those of free RSH. This line broadening observed in the solution NMR spectra of the thiol-derivatized gold nanoparticles is consistent with the alkyl chains being bound to the colloidal gold surface.[7] For example, in the ^{1}H NMR spectrum of the $C_{18}S$–Au colloid (Fig. 1A) the α, β, and γ methylene proton signals

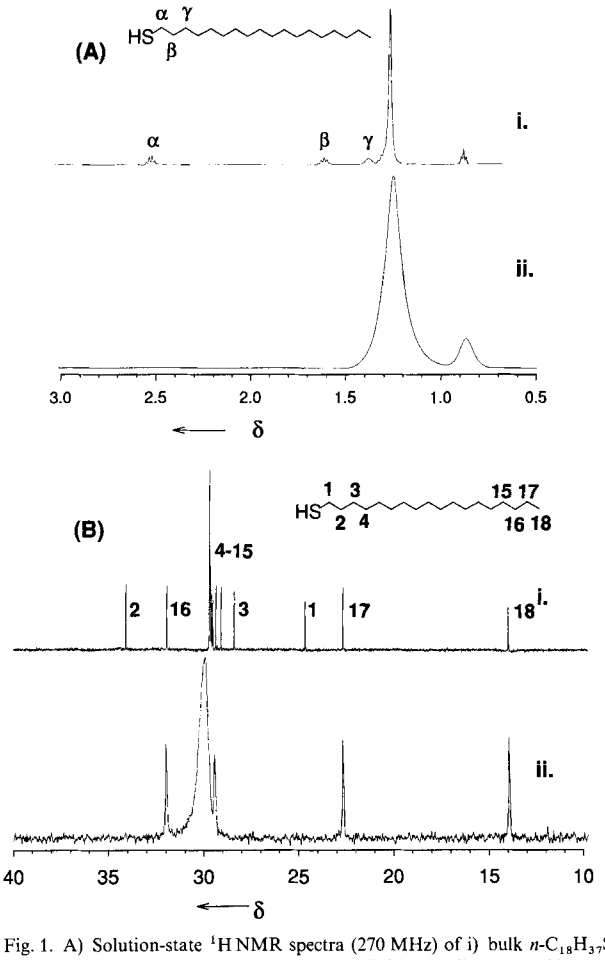

Fig. 1. A) Solution-state ^{1}H NMR spectra (270 MHz) of i) bulk n-$C_{18}H_{37}SH$ in $CDCl_3$, 64 transients and ii) $C_{18}H_{37}S$–Au colloid in [D_6]benzene, 128 transients. B) Solution-state ^{13}C NMR spectra (67.9 MHz) of i) bulk n-$C_{18}H_{37}SH$ in $CDCl_3$, 1024 transients and ii) $C_{18}H_{37}S$–Au colloid in [D_6]benzene, 13000 transients.

are noticeably absent, whereas the resonances associated with the C_4–C_{17} methylene hydrogens and the terminal methyl hydrogens are observed as broad signals. In the ^{13}C NMR spectrum (Fig. 1B), only the signals due to the carbons at positions 15–18 are clearly resolved, and the α, β, and γ carbons (i.e., the carbons closest to the gold surface) are not apparent. These signals may be buried under the broad peak at $\delta \approx 30$ (assigned to the interior methylene carbons of the alkylthiol chain), shifted by virtue of their binding to the metal, or more likely, broadened because of the "solidlike" nature of these carbons in the immobilized alkylthiol, as suggested elsewhere.[8]

TEM images (Fig. 2), in conjunction with elemental analyses, can be used to estimate the median coverage of thiols on the gold nanoparticles.[9] The synthetic procedure of Brust et al.,[6a] combined with our purification process, yields a coverage (assuming the particles to be spherical) at the gold surface corresponding to 17.2 ± 0.4 and 15.2 ± 0.4 Å^2 per alkylthiol molecule for the $C_{14}SH$- and $C_{18}SH$-derivatized Au colloid, respectively. A maximum packing density of these chains on a planar gold surface would require an area of 17.8 to 23.6 Å^2 per chain,[10] depending on the adsorption site (hollow or on-atom site) and the surface crystallography of the gold particle. Although these data are consistent with complete coverage by RSH, the ratio of the particle size to chain length precludes close packing of the chains along their entire length.[11] This restriction, imposed by the substantial curvature of the gold particle surface, leads to interesting particle–particle interactions, which in turn manifests itself in the temperature-dependence studies described below.

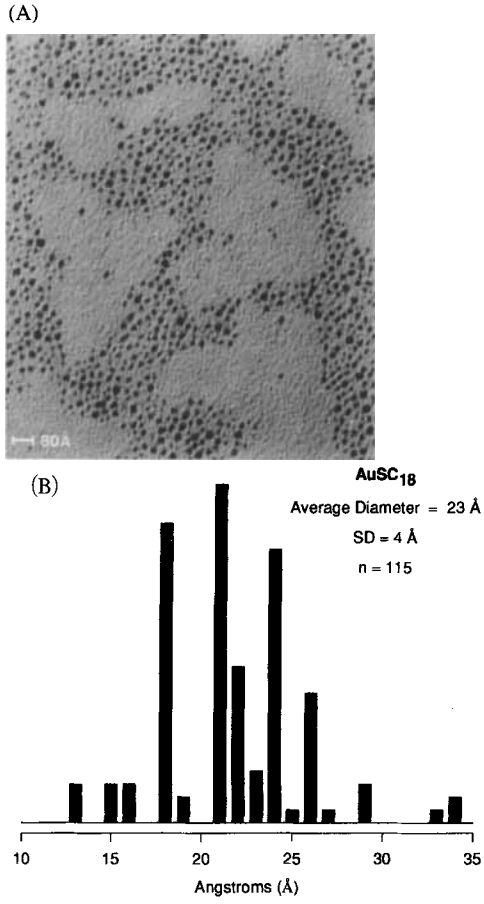

Fig. 2. A) Representative TEM image of $C_{18}SH$-derivatized Au nanoparticles. C_{12}, C_{14}, C_{16}, and C_{20} samples were similar to the C_{18} sample. B) Histogram of particle diameters observed in (A). Mean particle diameters, standard deviations, and the particle population size (n) are reported for each chain length; median diameters are given in parentheses. C_{12}: 19 ± 5 Å, $n = 103$ (18.5 Å); C_{14}: 20 ± 8 Å, $n = 126$ (21.4 Å); C_{16}: 29 ± 6 Å, $n = 108$ (28.0 Å), C_{18}: 23 ± 4 Å, $n = 115$ (22.4 Å), and C_{20}: 41 ± 14 Å, $n = 103$ (35.8 Å).

Variable-temperature NMR spectra of the dry powder samples, obtained on a liquid spectrometer, suggest that these alkylated nanoparticles undergo some form of melting transition. For instance, the ^{13}C NMR spectrum of the $C_{18}S$–Au powder

0947-6539/96/0203-0360 $ 15.00+.25/0 Chem. Eur. J. 1996, 2, No. 3

shows a broad weak signal between $\delta = 20-40$ at 25 °C (Fig. 3B). Between 55 and 65 °C a distinct peak ($\delta \approx 30$), assigned to the interior methylenes of the alkyl chain, appears and becomes relatively sharp. A signal consistent with the terminal methyl ($\delta \approx 15$) also becomes apparent at elevated temperatures. Furthermore, for the $C_{14}S-Au$ nanoparticles, the methylene signal is already apparent at 25 °C, and becomes substantially sharper (Fig. 3A) as the coated nanoparticles are heated to 45 °C. It is notable nonetheless, that there is a discernable population of mobile chains even at temperatures below the apparent phase-transition temperatures of these samples.[12] A detailed variable-temperature solid-state ^{13}C NMR examination of these samples has shown a gradual change in the population of *trans* to *gauche* conformers, consistent with the temperature-dependent data presented here.[8]

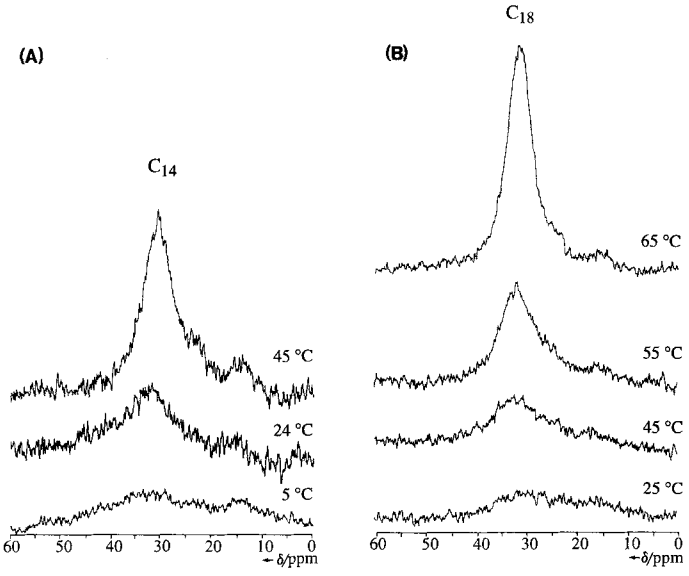

Fig. 3. Variable-temperature ^{13}C NMR (125 MHz) spectra of A) $C_{14}S-Au$ powder and B) $C_{18}S-Au$ powder; internal D_2O lock, 8400 transients.

Differential scanning calorimetry (DSC) of $C_{12}SH$-, $C_{14}SH$-, $C_{16}SH$-, $C_{18}SH$-, and $C_{20}SH$-derivatized gold nanoparticles quantifies the temperature dependence of the changes qualitatively observed by NMR. Each sample exhibits a broad endotherm (or a set of overlapping endotherms) in the heat cycle (Fig. 4A). The temperature of the peak maximum is clearly dependent on chain length, and the ΔH associated with this transition increases with increasing chain length. This trend parallels that seen in materials undergoing gel-to-liquid crystalline transitions, given that an increasing chain length affords more extensive van der Waals interactions and resulting enthalpic contributions. On cooling, a sharp exotherm is observed at approximately 7 °C below the endotherm (Fig. 4B). Although this hysteresis behavior is observed with all RS–Au samples studied, the thermal processes are evidently reversible given that the $\Delta H_{endo} = \Delta H_{exo}$. Upon reheating the cooled nanoparticles, a sharper endotherm results owing to annealing of the alkylated particles. However, the enthalpies and peak-maximum temperatures remain the same (i.e., $\Delta H_{heat} = \Delta H_{reheat}$, $\Delta T \approx 2$ °C); this indicates that the DSC-detected transition is reversible. Clearly, since the thermograms are reversible, thiol desorption does not compete with the thermal properties of the alklylated particles at temperatures ≤ 95 °C.[13] The DSC thermograms clearly show that these RS–Au particles, in the solid state, undergo

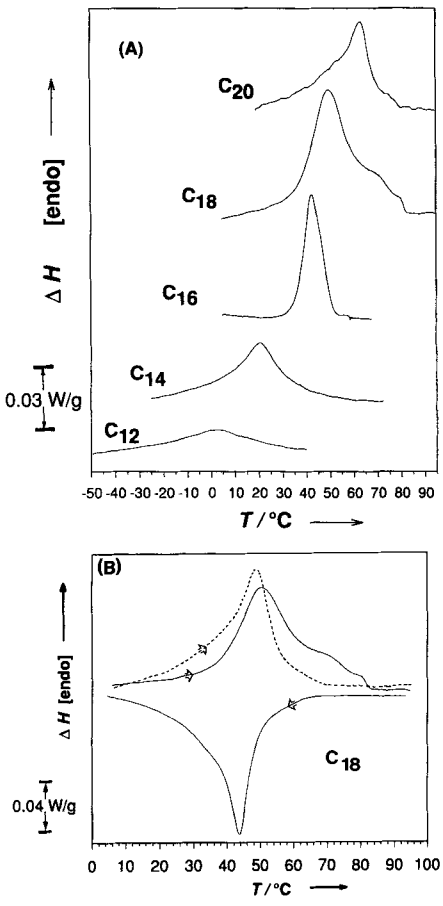

Fig. 4. A) Differential scanning calorimetry endotherms of RS–Au powders. Heat cycle, scan rate 5 °C min^{-1}, except for $C_{20}S-Au$, 2 °C min^{-1}. B) Heat (⇒), cool (⇐), reheat (⇒) cycling of a $C_{18}S-Au$ sample.

distinct phase transitions in a chain length dependent manner. The transition temperature associated with each chain closely parallels those found in both electrochemical SAM studies,[4] and in classic studies of phospholipid (PC) bilayer membranes (Table 1).[14]

FT-IR spectroscopy used in conjunction with NMR and DSC provides information concerning the conformation of chains adsorbed to surfaces. For example, surface infrared spectroscopy (i.e., reflection absorption infrared spectroscopy, RAIRS) has been used to probe the chain conformation and orientation of thiol SAMs on planar gold.[15] However, the dispersed nature of the gold nanoparticle system allows us to use conventional transmission FT-IR, with the sample deposited as a thin film on an inert substrate. For example, Figure 5 tracks the CH_2 symmetric (d^+: 2850 cm^{-1}) and antisymmetric (d^-: 2920 cm^{-1}) stretches of $C_{18}S-Au$ as a function of temperature. Figure 6 thus shows that upon heating, the $C_{14}S$-, $C_{16}S$-, and $C_{18}S-Au$ samples undergo a transition from a highly chain-ordered state to a chain-disordered state, where the CH_2 symmetric (d^+: 2850 cm^{-1}) and antisymmetric (d^-: 2920 cm^{-1}) stretches are used as markers of *trans* and *gauche* bond populations in the chains.[2, 16] Although this process occurs over a relatively broad temperature range (≈ 25 °C), as is the case in the NMR and calorimetry experiments (Figs. 3 and 4), the apparent transition temperatures are similar to those found by other techniques reported here. Also notable is the observation that the population of *gauche* bonds at 25 °C follows the trend of $C_{14} > C_{16} > C_{18}$. This is consistent with a differing extent of chain disordering in the samples when they are observed near to,

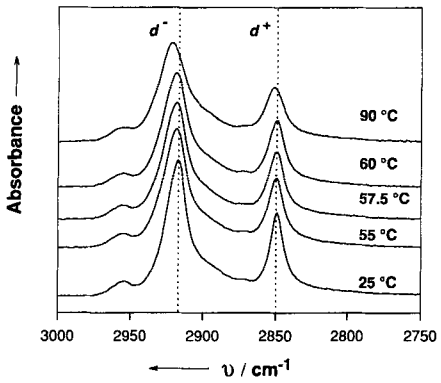

Fig. 5. Variable-temperature transmission FT-IR spectra of the CH_2 stretching region (2750–3000 cm^{-1}) for $C_{18}S$–Au particles. The dotted lines at 2917 and 2850 cm^{-1} are visual aids.

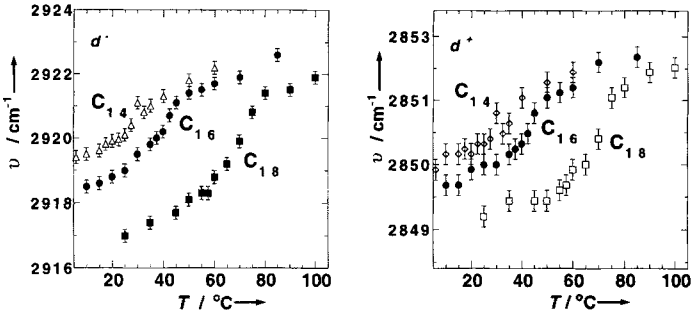

Fig. 6. Peak position of the antisymmetric (d^-) and symmetric (d^+) CH_2 stretches as a function of temperature for RS–Au powders of $C_{14}S$-, $C_{16}S$-, and $C_{18}S$–Au nanoparticles deposited on a NaCl crystal.

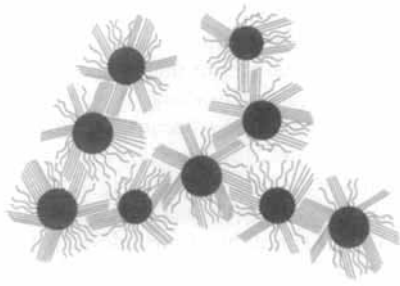

Fig. 7. Schematic two-dimensional representation of the RS–Au nanoparticles in the solid state, as suggested by the data shown in Figures 1–6. In this description, a number of chain domains on a given gold particle will interdigitate into the chain *domains* of neighboring particles in order to compensate for the substantial decrease in the chain density which occurs towards the methyl chain end. Chains with large populations of *gauche* bonds may arise from i) those which occupy *interstitial* regions in the particle lattice and cannot efficiently overlap with adjacent chains or from ii) chains residing at domain boundaries. An alternative packing configuration, involving the interdigitation of individual chains from neighboring particles, is not likely given the large chain end to surface area ratio [11].

Table 1. A comparison of the thermal properties of self-assembled films.

	RS–Au nanoparticles			Planar RS–Au	Di-PC lipids	
	T_m^{DSC}/°C [a]	ΔH [b]	T_m^{IR}/°C [c]	T_m^e/°C [d]	T_m/°C [e]	ΔH/kJ mol^{-1}
C_{12}	3	(5)	–	–	−1.1±0.4	–
C_{14}	22	10 (11)	24	–	23.5±0.4	24.7±2.7
C_{16}	41	(12)	42	39.3±0.6	41.4±0.5	–
C_{18}	51	21 (23)	66	53.3±2.4	55.1±1.5	42.3±3.7
C_{20}	64	(30)	–	62.8±1.8	64.5±0.5	–

[a] T_m^{DSC} refers to the peak-maximum temperature of the endotherm in the first heat cycle. [b] ΔH is reported in J g^{-1} of RS–Au powder (values in parentheses) and in kJ mol^{-1} of alkylthiol for the samples subjected to elemental analyses. [c] Inflection points of these plots were determined by taking the second derivative of the best-fit polynomial in each case, and are used as apparent T_m values reported by FT-IR spectroscopy. [d] T_m^e values determined electrochemically for alkylthiols adsorbed on planar gold [4]. [e] T_m values of *n*-diacylphosphatidylcholine lipids determined by DSC [14].

or distant from, the DSC-determined phase-transition temperature. These data are especially interesting, since several studies using RAIRS of RSH monolayers on planar gold substrates in UHV conditions have failed to detect phase transitions through the temperature dependence of either the d^+ or d^- CH_2 stretching peaks, which would otherwise be indicative of order–disorder transitions.[16]

The DSC and FT-IR experiments establish that a cooperative chain-melting process occurs in these alkylated metal colloids, the mechanism of which is not immediately evident given the relationship between the extended chain conformation and the gold nanoparticle geometry. Extensive chain–chain interactions may arise in two ways, assuming a variation in density of the adsorbed surfactant. Chains may collectively tilt to form close-packed domains. Detailed diffraction studies established that RSH chains chemisorbed on planar Au(111) are tilted by about 30° with respect to the surface normal so as to maximize van der Waals interactions.[10] While this may in fact occur in the thiol-modified nanoparticles, close examination of TEM micrographs suggests that chain ordering arises from the interdigitation of chain *domains* between neighboring particles (Fig. 7). Given that TEM images the gold nanoparticle, and not the organic adsorbate, the distances between the edges of many pairs of adjacent particles (Fig. 2) clearly are substantially less than twice an all-*trans* extended chain length, and indeed, are closer to being one chain in length (i.e., ≈20 Å).

An interdigitated state is interesting in that the void-filling process leads to a bilayerlike configuration of chains. Phase-transition temperatures (T_m's) reflect the extent of van der Waals interactions, which depend on the chain-packing density. Thus, the agreement between the T_m values of planar RS–Au SAMs (determined electrochemically),[4] phospholipid bilayers,[14] and RS–Au nanoparticles suggests that these order–disorder processes are structurally related. Changes in chain ordering could lead to broadening of the phase transitions and may cause shifts in the observed T_m values. The RS–Au nanoparticle T_m would also be influenced by the packing state of the RSH chains in the modified gold nanoparticles. In a related system, a C_{12}-derivatized C_{60} fullerene (d = 11.3 Å) exhibits a phase transition at ≈ 24 °C (measured by DSC). In this particular case, an interdigitated phase was determined by X-ray diffraction, and is thought to be the source of the observed phase transition.[17]

Conclusion

These studies show that RS–Au nanoparticles can be prepared with monolayer coverage of the gold particles. They then have the same physical and chemical properties as thiol monolayers. An order–disorder transition is readily monitored by FT-IR spectroscopy and NMR spectroscopy,[8] and this transition correlates with DSC-detected endotherms. This thermally induced transition is associated with structural changes in the organic monolayer coating, given the distinct dependence of the phenomenon on chain length. Distinct phase transitions are detectable in these organic films; this suggests that the RS–Au nanoparticle can be considered to be a highly dispersed, large surface area analogue to the much-studied self-assembled thiol monolayers on planar gold. It is important to note that neither

0947-6539/96/0203-0362 $ 15.00+.25/0 Chem. Eur. J. 1996, 2, No. 3

the calorimetry nor NMR experiments can be performed, at present, on SAMs supported on planar surfaces. The research presented here paves the way for the extension of a number of the biomimetic and optical applications being undertaken with RS–Au SAMs to these readily prepared colloidal systems.

Experimental Procedure

Materials: C_{12}-, C_{14}-, C_{16}-, C_{18}-, and C_{20}SH were prepared and purified as previously described [4]. Hydrogen tetrachloroaurate trihydrate, sodium borohydride (99%), and tetraoctylammonium bromide (98%) were obtained from Aldrich and used as received.

Synthesis: Gold nanoparticles derivatized with alkylthiols of chain lengths of 12, 14, 16, 18, and 20 carbons were prepared following the method of Brust et al. [6a]. This procedure involves two phases (toluene/water), where $Au^{III}Cl_4^-$ is transferred to the toluene layer with $(C_8H_{17})_4NBr$ as a phase transfer reagent, and then reduced by $NaBH_4$ in the presence of the thiol surfactant at the toluene/water interface. The reactions were carried out under ambient atmosphere typically with 1.8 mmoles of $HAuCl_4 \cdot 3H_2O$ and mole ratios of $NaBH_4$:$(C_8H_{17})_4NBr$:$HAuCl_4$:RSH of 12:4.8:1.1:1. Rigorous purification of the RS–Au colloid was found to be necessary as both the original preparation and the recrystallized sample showed large amounts of residual thiol and disulfide. Exhaustive washing/extraction of the colloid preparation with ethanol served to quantitatively remove unbound species. Complete removal of residual thiol and disulfide was verified by TLC using hexane as the mobile phase and iodine as the indicator. The final purified material used in calorimetry and spectroscopy experiments is a finely divided, crystalline (for $n \geq 16$) or waxy ($n \leq 14$) brown-black powder, which remains as a solid pellet in water, yet disperses to yield a colloidal solution in solvents such as hexane, benzene, toluene, and chloroform [6a]. Two samples of RSH-derivatized gold were subjected to elemental analysis (Galbraith Laboratories, Knoxville, USA). $C_{14}H_{29}S$–Au nanoparticles yield 75.67% Au, 3.40% S, 18.30% C, and 3.03% H, while the $C_{18}H_{37}SH$-derivatized Au nanoparticles yield 69.32% Au (by difference), 3.33% S, 23.49% C, and 3.86% H.

Transmission electron microscopy: Samples for TEM were prepared by dipping standard carbon-coated (200–300 Å) Formvar copper grids (200 mesh) into a dilute hexane solution of the RS–Au nanoparticles for several seconds. The TEM grids were withdrawn from the solution and allowed to dry under ambient atmosphere for a few minutes. Phase contrast images of the particles were obtained with a top-entry Phillips EM410 electron microscope operated at an accelerating voltage of 80 keV. Micrographs were obtained at magnifications of 52000× and 92000×. The size distributions of the various RS–Au nanoparticles were determined from the diameters of at least 100 particles located in a representative region of the 17× enlarged micrographs using a video image analysis software program (JAVA, Jandal Scientific).

NMR spectroscopy: Solution state NMR experiments were performed on a JEOL ECLIPSE-270 spectrometer at 25°C, on samples prepared by dispersion of 30–40 mg of the RSH-derivatized Au colloid in 0.7 mL of [D_6]benzene. Variable-temperature ^{13}C NMR of the $C_{14}S$- and $C_{18}S$–Au powders were carried out on a Varian Unity 500 NMR spectrometer using D_2O coaxial insert as a field/frequency lock. ^{13}C NMR measurements were performed under conditions of broadband ^1H decoupling. The proton and the ^{13}C resonances are reported in ppm vs. TMS.

Infrared spectroscopy: The RS–Au colloidal particles were deposited dropwise onto a NaCl disc from a concentrated hexane solution. Except for the $C_{20}H_{41}S$–Au case, evaporation of the solvent resulted in a uniform film. Infrared spectroscopy was carried out with a Perkin-Elmer FT-IR Microscope Model 16PC with a MCT detector. Spectra were collected in the transmission mode with an unpolarized beam, at a resolution of 2 cm^{-1} with 32 scans, and a spectral window from 4000 to 600 cm^{-1}. The FT-IR microscope was equipped with a Mettler FP52 hot stage for variable-temperature experiments (5–100°C). The sample was purged continuously with dry nitrogen and maintained at each temperature for 30 min before a spectrum was acquired. Background spectra of the clean NaCl disc were collected at the same temperatures and subtracted from the sample spectra.

Differential scanning calorimetry: DSC experiments were conducted with a Perkin-Elmer DSC-7 instrument calibrated for temperature and peak area by means of indium and octadecane standards. Thermograms were run on samples of 2–8 mg of a RS–Au colloid in sealed aluminum pans under a nitrogen atmosphere at heat–cool rates ranging from 2 to 5°C min^{-1}.

Acknowledgments: This work was supported by the Natural Sciences and Engineering Research Council of Canada and by the Canadian Bacterial Diseases Network Center of Excellence. We would like to thank P. M. Peters for performing the initial solution-state NMR measurements, and Prof. L. Reven for helpful discussions.

Received: September 7, 1995 [F251]

[1] A. Ulman, *An Introduction to Ultrathin Organic Films from Langmuir–Blodgett to Self-Assembly*, Academic Press, San Diego, CA, **1991**; C. D. Bain, G. M. Whitesides, *Angew. Chem. Adv. Mater.* **1989**, *101*, 522; *Angew. Chem. Int. Ed. Engl. Adv. Mater.* **1989**, *28*, 506, and references therein.

[2] L. H. Dubois, R. G. Nuzzo, *Annu. Rev. Phys. Chem.* **1992**, *43*, 437, and references therein.

[3] J. Lipkowski in *Modern Aspects of Electrochemistry*, *Vol. 11*, Plenum, N. Y., USA.

[4] A. Badia, R. Back, R. B. Lennox, *Angew. Chem.* **1994**, *106*, 2429; *Angew. Chem. Int. Ed. Engl.* **1994**, *33*, 2332.

[5] P. Fenter, P. Eisenberger, K. S. Liang, *Phys. Rev. Lett.* **1993**, *70*, 2447.

[6] a) M. Brust, M. Walker, D. Bethell, D. J. Schriffin, R. Whyman, *J. Chem. Soc. Chem. Commun.* **1994**, 802; b) D. V. Leff, P. C. Ohara, J. R. Heath, W. M. Gelbart, *J. Phys. Chem.* **1995**, *99*, 7036.

[7] E. Söderlind, P. Stilbs, *Langmuir* **1993**, *9*, 1678.

[8] A. Badia, W. Gao, S. Singh, L. Demers, L. Cuccia, L. Reven, *Langmuir*, in press.

[9] Elemental analyses, in conjuction with the median diameters of the gold nanoparticles were used to determine thiol coverage. The median diameter rather than the mean diameter was used since it more accurately reflects the size of an idealized particle, as seen in Figure 2. However, the median and mean diameters were found to be similar. The $C_{14}S$–Au colloid of 21.4 Å diameter resulted in a coverage of 84 ± 2 $C_{14}S$- chains per Au nanoparticle, and a corresponding area per chain of 17.2 ± 0.4 Å^2. $C_{18}S$–Au, of particle diameter 22.4 Å, gave a coverage of 104 ± 3 $C_{18}S$- chains per Au nanoparticle, and an area per chain of 15.2 ± 0.4 Å^2, which is comparable to the van der Waals area per chain of ca. 15.9 Å^2. These coverages correspond to a surface Au to thiol ratio of ca. 2.5:1 (C_{14}) and 2.2:1 (C_{18}). Heath et al. calculated a ratio of ca. 2:1 surface Au to thiol for C_{12}SH-derivatized Au nanoparticles of 20 Å [6b] in diameter.

[10] N. Camillone, C. E. D. Chidsey, G. Liu, G. Scoles, *J. Chem. Phys.* **1991**, *94*, 8493, and references therein.

[11] For example, a colloid (d = 22 Å) whose $C_{18}H_{37}SH$ area is 18 Å^2 and all-*trans* extended chain length is 29.8 Å would provide an area per chain end that is 14-fold greater.

[12] Dispersion of the nanoparticles in a good solvent (i.e., benzene, toluene, $CHCl_3$) leads to a disordering or solubilization of the chains on the particle. This is evident in solution-state NMR studies, where the spectra become relatively well-resolved and narrow-lined, indicative of a highly mobile state. Any solvent which allows the isolation of the RS–Au particles in solution will most likely also solvate the alkyl chains and disrupt chain–chain interactions; the net result is an absence of any phase-transition behavior in the temperature region probed in Figures 3 and 4.

[13] Temperature-programmed desorption studies of a hexdacanethiol monolayer chemisorbed on a Au(111) single-crystal surface show that desorption of the thiol occurs at $T \geq 227$°C [15a].

[14] D. Marsh, *Handbook of Lipid Bilayer Membranes*, CRC, Boca Raton, FL, **1991**.

[15] a) R. G. Nuzzo, L. H. Dubois, D. L. Allara, *J. Am. Chem. Soc.* **1990**, *112*, 558; b) P. E. Laibinis, G. M. Whitesides, D. L. Allara, Y.-T. Tao, A. N. Parikh, R. G. Nuzzo, *ibid.* **1991**, *113*, 7167; c) M. D. Porter, T. B. Bright, D. L. Allara, C. E. D. Chidsey, *ibid.* **1987**, *109*, 3559.

[16] a) L. H. Dubois, B. R. Zegarski, R. G. Nuzzo, *J. Electron Spectrosc. Relat. Phenom.* **1990**, *54/55*, 1143; b) R. G. Nuzzo, E. M. Korenic, L. H. Dubois, *J. Chem. Phys.* **1990** *93*, 767; c) F. Bensebaa, T. H. Ellis, A. Badia, R. B. Lennox, *J. Vac. Sci. Technol. A* **1995**, *13(3)*, 1331, and references therein.

[17] K. Levon, D. Weng, J. Mao, H. K. Lee, J. M. Tour, W. A. Schrivens, *Mat. Res. Soc. Symp. Proc.* **1994**, *349*, 127.